Irregular heat source and non-linear convective Heat & mass transfer in Hybrid nano material passed through concentric cylinder

Indira S[1], Nalinakshi N[1], Sreenivasa T N[2], Dinesh P A[3]

[1]Department of Mathematics, Atria Institute of Technology, Bengaluru, KA, India
[2]Department of Mechanical Engineering, Atria Institute of Technology, Bengaluru, KA, India
[3]Department of Mathematics, MS Ramaiah Institute of Technology, Bengaluru, Karnataka, India

Abstract:

An analysis of convective heat and mass transfer of nanofluids flow that are connected to an annulus-shaped, two concentric cylindrical regions are studied. The hybrid nanoparticles in Cu-Au and water-based hybrid nano liquids are considered, the salient features of convection in an inclined porous annulus are analysed. The conservation laws are in a non-linear model for the geometry considered. Using the appropriate analogues transformations, the resultant equations are employed RK-4th order method with shooting technique to obtain closed form solutions for transverse velocity, temperature, and concentration. The consequences of key parameters on the non-dimensional velocity, temperature, concentration, skin friction coefficient are presented through surface plots. The second order resistance and mixed convection mechanisms favours the flow structure. The velocity, temperature and concentration fields are greater for platelet-shaped nanoparticles, when compared to cylinder, bricks, and spherical-shaped nanoparticles. Applications of cylinders in nuclear waste disposal, energy extraction in catalytic beds. The observations of the present investigation are in good agreement with the flow structure of various physical parameters with the existing ones.

Keywords: Laminar flow, irregular heat source, hybrid nanoliquid, Heat and mass transfer, porous medium, concentric cylinder

Introduction:

Mixed convection is a phenomenon that can happen in electronic equipment like computer chips. While natural convection can happen because of temperature differences, forced convection can be produced by fans or heat sinks. Mixed convection is frequently used in HVAC (heating, ventilation, and air conditioning) systems. Fans can force air over an area, but convection from the natural environment can also distribute heat. Mixed convection is a common occurrence in solar collectors, which are devices that capture solar energy. Both forced and natural convection can be induced by temperature variations brought about by the absorbed solar energy. Mixed convection can occur in a variety of industrial operations using heat exchangers. For instance, forced convection via a pump and spontaneous convection from temperature gradients are both possible in a chemical reactor. Systems for ventilating buildings may combine natural convection with forced air movement. This is especially important in areas where ventilation and temperature requirements vary. Designing effective heat transfer systems requires an understanding of the ability to forecast mixed convection. Computational fluid dynamics (CFD) simulations are widely used by researchers and engineers to study and improve systems in which mixed convection plays a key role. This enhances the effectiveness and energy economy of numerous applications pertaining to heat transfer and fluid flow.

Researchers have been paying close attention to heat transfer enhancement in engineering and industrial applications in the last several years. This is because the rate of

heat transfer has a major impact on the efficiency of most of the equipment used in this industry, such as heat exchangers and electrical devices. Because of their low thermal conductivity, base fluids like water, oil, and ethylene glycol limit the pace at which heat is transferred. One kind of nanosized particle is added to the a fore mentioned fluids to make up for their deficit. Choi and Eastman [1] initially discussed this procedure and referred to this mixture as "nanofluid" and the pioneers of this novel form of nanotechnology. The researchers have examined a wide range of nanoparticle combinations, including semiconductors (SiO_2, TiO_2), metal oxides (Al_2O_3, CuO).

Although there are so many possible uses for nanoparticles in the optical, biological, and electronic fields, there is currently a strong scientific interest in this sector. A particle is defined in nanotechnology as a microscopic object that functions in terms of attributes and transport. The field of nanotechnology encompasses the development and use of materials with nanoscale sizes between 1 and 100 nm to produce goods with unusual characteristics. The use of nanotechnology in biological applications with distinctive physical and chemical properties has the potential to produce greatly enhanced molecular liability devices and diagnostic techniques [2–3]. Afterwards, in an asymmetric channel, Akbar et al. [4] study the effect of metallic nanoparticles on incompressible viscous fluid. In a curved tube, the two phase nanofluid was examined by Nadeem et al. [5]. Researchers have given special attention to nanoparticles, and several studies have been conducted to examine the benefits of nanotechnology in a range of applications. These studies are published in literature and can be found in sources like [6–7]. An extremely important tool for studying the origins of many complications in human organs where peristaltic pumping is used, such as the stomach and small intestine, is the endoscope. Moreover, the distribution and flow inside an artery will alter because of a catheter injection. Numerous inquiries are conducted to Examine how the endoscope affects both Newtonian and non-Newtonian fluids' peristaltic transit [8-9].

Applications of nanofluids plays a novel role in heat transfer technique using hybrid nanofluids has recently gained popularity among scientists, engineers, and researchers. The concept and development of nanofluids—basic fluid with nanoparticles—were groundbreaking. When several different nanoparticles are combined to form a homogenous phase, this process is referred to as "hybridization." The typical materials of the nanoparticles that are disseminated in kerosene, water, ethylene glycol, and oil are metals (Al, Fe, and Cu), metal oxides (MgO, Al_2O_3, and CuO), semiconductors (SiO_2), and TiO_2. Suresh and associates [10] shown that improved thermophysical properties can be seen when metallic and non-metallic nanoparticles are combined with a conventional liquid. They demonstrated that the thermal hybrid nanoliquids (Al_2O_3-Cu-H_2O) diffusivity is greater than the mono Nano liquids. Devi and Devi [11] investigated a numerical analysis of hybrid nano liquid flow past a plate with a Newtonian heating effect. They demonstrated that Cu - Al_2O_3/water had a higher heat transfer rate than Cu/water. The stability and heat transfer mechanism of a water-based hybrid nanoliquid was investigated by Kanchana et al. [12] explained isothermal border restrictions. The suspension of two nanoparticles in water is shown to result in an improvement in the friction factor. Sathya Narayana and Venkateswarlu [13] investigated the magnetized hybrid nanoliquid flow across an extended plate with THS and conclude that, in terms of flow structure and thermal pattern, hybrid nanoliquids are more important than nanoliquids. Using hybrid nanoliquid, Waini et al. [14] investigated the impact of the porous media on mixed convective flow. They demonstrated how the dispersion of nanoparticles reduces the boundary layer separation.

It is of interest to study the effect of heat source on temperature distributions and heat transfer when the fluid is capable of emitting and absorbing thermal radiation. Over the years, due to the use of cylinders in nuclear waste disposal, energy extraction in catalytic beds, and undergrounds, convective heat transfer about cylindrical geometries has begun to attract the attention of many researchers. This can be explained by the fact that, when considering space applications (space travel) and higher operating temperatures, heat transmission by thermal radiation is becoming more significant. Numerous writers have examined heat generation and thermal radiation in cylindrical shape. The heat and mass transmission of an MHD flow over a moving object was examined by Chamkha [15]. permeable cylinder capable of chemical reaction, heat generation, or absorption. He concluded that the fluid velocity is decreased by the Hartmann number. The heat and mass transfer process during the evaporation of water from a circular surface. cylinder by means of CFD simulation. The heat and mass transport from a permeable cylinder in a porous medium with heat generation/absorption as well as a magnetic field in other related study. The investigated an unsteady natural convective flow past semi-infinite vertical cylinder with heat and mass transfer under different physical situations. Using an implicit finite-difference technique, [16-17] described the radiation-conduction interaction on mixed convection from a horizontal circular cylinder.

Approximation of Boussinesq (NBA). According to their analysis, the NBA is advantageous for the flow field. Kameswaran et al. [18] examined the quadratic convective flow in a wave-shaped surface filled with Nano liquid. Looked at the heat transfer characteristic over a plate using the NBA. According to their analysis, the NBA has a higher flow structure than the LBA. A recent statistical examination of hybrid Nano liquid flow in an annulus subjected to NBA was carried out by Thriveni and Mahanthesh [19]. They discovered that NBA accounting increases heat transfer. Conversely, not much research has been done on the effect of NBA on the flow of hybrid nanoliquid in a convectively heated inclined porous annulus.

This paper addresses the dynamics of hybrid nanoliquids in a convectively heated inclined porous annulus under nonlinear Boussinesq approximation, based on a survey of the literature and hybrid nanoliquid applications. The analysis of heat and mass transfer over a concentric cylinder in the presence of Cu-Au nanoparticles. The impacts of THS and ESHS is another innovative feature of this work. The bvp5c routine is used to obtain the numerical solutions for the complex governing equations. Examined further is the impact of effective parameters on flow characteristics.

Mathematical formulation:

The nonlinear mixed convection of Cu-Au H_2O hybrid nanoliquid in an inclined porous annulus is considered. the convective boundary conditions $k_{hnl}\frac{\partial T}{\partial r} = h_1(T - T_0)$ at inner cylinder and $k_{hnl}\frac{\partial T}{\partial r} = -h_2(T - T_W)$ at outer cylinder are considered. The standard cylindrical coordinate system is taken into consideration, with the z-axis serving as the annulus' common axis and the r-axis pointing in the radial direction. Since the fluid flow is independent of z due to the annulus of infinite length, the interested domine is defined by the r-axis, where the radius of the inner cylinder a is less than the radius of the outer cylinder b. The fluid obeys the nonlinear Boussinesq approximation and is incompressible, Newtonian, and heat-conducting. The Darcy law for the porous medium, THS, and ESHS features is used to characterize the heat transfer rate and flow structure. Included are not the effects of Joule heating, induced magnetic field, or viscous dissipation. The governing equation for laminar flow inside the annulus is given below [19-20]
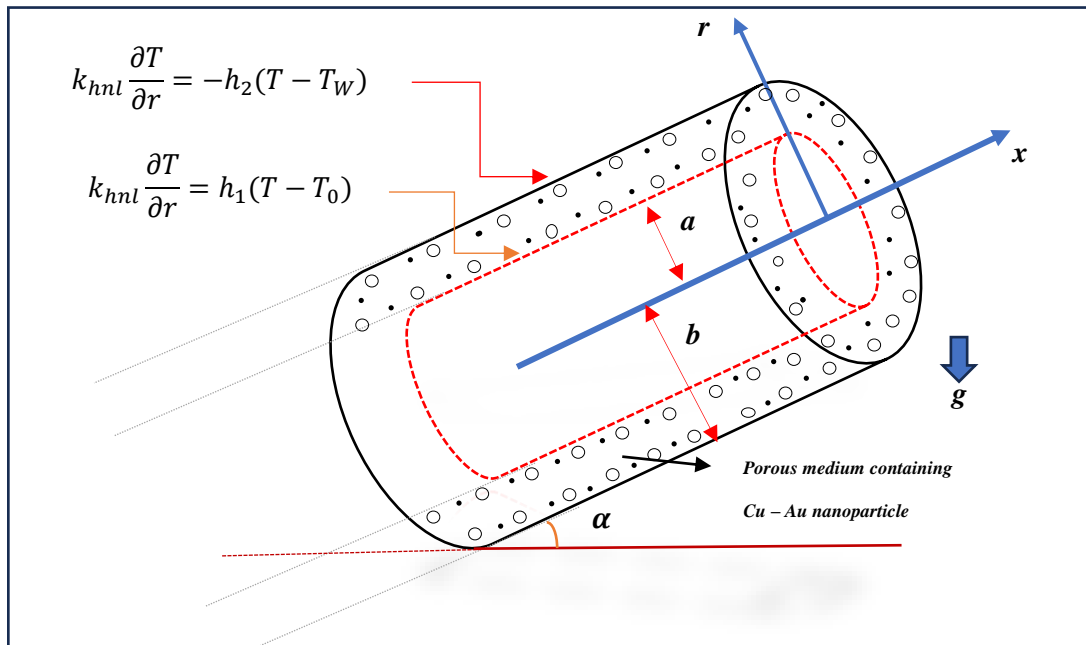
Fig 1: Physical arrangement of the problem.

Conservation of momentum

$$\frac{\mu_{hnl}}{\rho_{hnl}} \cdot \frac{1}{r}\frac{d}{dr}\left(r\frac{du}{dr}\right) + \frac{g}{\rho_{hnl}}[(\rho\beta_0)_{hnl}(T-T_0) + (\rho\beta_1)(T-T_0)^2]cos\alpha - \frac{g}{\rho_{hnl}}[(\rho\gamma_0)_{hnl}(C-C_0) + (\rho\gamma_1)(C-C_0)^2]cos\alpha + u^*\frac{\mu_{hnl}}{K,\rho_{hnl}} - \frac{1}{\rho_{hnl}}\frac{dP}{dZ} = 0 \tag{1}$$

Conservation of energy

$$\frac{K_{hnl}}{(\rho C_p)_{hnl}}\left[\frac{1}{r}\frac{d}{dr}\left(r.\frac{dT}{dr}\right)\right] + \frac{Q_0}{(\rho C_p)_{hnl}}(T-T_0) + \frac{(T_w-T_0)}{(\rho C_p)_{hnl}}Q_l exp\left(\frac{-nr}{a}\right) = 0 \tag{2}$$

Concentration equation

$$\frac{D_B}{r}\frac{d}{dr}\left(r\frac{dc}{dr}\right) - K(C-C_0)^n = 0 \tag{3}$$

under the boundary conditions

$$r = a\,; u' = 0, \qquad k_{hnl}\frac{\partial T}{\partial r} = h_1(T-T_0), k_{hnl}\frac{\partial C}{\partial r} = d_1(C-C_0)$$

$$r = b\,; u' = 0, k_{hnl}\frac{\partial T}{\partial r} = -h_2(T-T_W), \ k_{hnl}\frac{\partial C}{\partial r} = -d_2(C-C_W) \tag{4}$$

where u' denotes the velocity, ρ −density, T-temperature, g-acceleration due to gravity, α −angle of inclination, Q_0 −THS co-efficient, K permeability factor, Q_E −ESHS co-efficient, k-thermal conductivity, n-exponential index, v-viscosity and C_p-heat capacitance (h_1, h_2)- convective heat transport co-efficient. (d_1, d_2) −convective mass transfer co-efficient. The subscript *hnl*- hybrid nano liquid *and l* -base liquid.

The total nanoparticle volume fraction is defined as;

$$\emptyset = \emptyset_{Cu} + \emptyset_{Au} \tag{5}$$

The effective thermophysical properties of hybrid nano liquid is given by mixed theory [21-22]

$$(\rho\beta_0)_{hnl} = \left((1-\emptyset) + \emptyset_{Cu}\frac{(\rho\beta_0)_{Cu}}{(\rho\beta_0)_l} + \emptyset_{Au}\frac{(\rho\beta_0)_{Au}}{(\rho\beta_0)_l}\right)(\rho\beta_0)_l, \tag{6}$$

$$(\rho\gamma_0)_{hnl} = \left((1-\emptyset) + \emptyset_{Cu}\frac{(\rho\gamma_0)_{Cu}}{(\rho\gamma_0)_l} + \emptyset_{Au}\frac{(\rho\gamma_0)_{Au}}{(\rho\gamma_0)_l}\right)(\rho\gamma_0)_l, \tag{7}$$

$$\rho_{hnl} = \left((1-\emptyset) + \emptyset_{Cu}\frac{\rho_{Cu}}{\rho_l} + \emptyset_{Au}\frac{\rho_{Au}}{\rho_l} \right)\rho_{l\prime} \tag{8}$$

$$(\rho C_p)_{hnl} = \left[(1-\emptyset) + \frac{\emptyset_{Cu}(\rho C_p)_{Cu}}{(\rho C_p)_l} + \frac{\emptyset_{Au}(\rho C_p)_{Au}}{(\rho C_p)_l} \right](\rho C_p)_{l\prime} \tag{9}$$

The brinkman model for the effective dynamic viscosity is given by phenomenological law [19]

$$\mu_{hnl} = \frac{1}{(1-\emptyset)^{2.5}}\mu_{l\prime} \tag{10}$$

The effects of several nanoparticle forms, including spherical, platelet, cylinder, and brick, has been examined in this work using the Hamilton-Crosser model for effective thermal conductivity. The results are provided by

$$\frac{k_{hnl}}{k_l} = \frac{\left(\frac{(\emptyset k)_{Cu}+(\emptyset k)_{Au}}{\emptyset}\right)+(m-1)k_1+(m-1)((\emptyset k)_{Cu}+(\emptyset k)_{Au})-(m-1)k_l\emptyset}{\left(\frac{(\emptyset k)_{Cu}+(\emptyset k)_{Au}}{\emptyset}\right)+(m-1)k_l-((\emptyset k)_{Cu}+(\emptyset k)_{Au})+k_l\emptyset} \tag{11}$$

In this case, the subscript the form factor is m, and the copper and gold nanoparticles are Au and Cu. The hybrid nano liquid's thermophysical characteristics and form factor values are tabulated.

Dimension less equations are [19]

$$U = \frac{\mu}{\mu_0}, P = \frac{pa}{u_0 v_l},$$

$$\theta = \frac{T-T_0}{T_w-T_0}, R = \frac{r}{a}, Z = \frac{z}{a} \; ; C = \frac{C-C_0}{C_w-C_0} \tag{12}$$

By virtue of equation no (12) and (5) to (11). The equations (1)-(4) reduced to the following equation

$$\frac{d^2u}{dR^2} = \frac{U}{D_a} + \frac{M}{A_1} - \frac{1}{R}\frac{du}{dR} - \frac{Mc}{A1}[A_2\theta + Q_c.\theta^2]cos\alpha \tag{13}$$

$$\frac{d^2\theta}{dR^2} = \frac{-1}{R}\frac{d\theta}{dR} - Q_T\frac{\theta.Pr}{A_4} - \frac{Pr}{A_4}.Q_E.exp(-nr) \tag{14}$$

$$\frac{d^2\phi}{dR^2} = \frac{-1}{R}\frac{d\phi}{dR} + K.S_c.\phi \tag{15}$$

At $R = 1: U = 0, \frac{d\theta}{dR} = \frac{Bi_1}{A_4}\theta$; $R = \lambda: U = 0, \frac{d\theta}{dR} = \frac{Bi_2}{A_4}(1-\theta)$

At $R = 1: \frac{d\phi}{dr} = \frac{Di_1}{K_{nl}}\phi; R = \lambda = \frac{b}{a}, \frac{d\phi}{dr} = \frac{-Di_2}{K_{nl}}(1-\phi) \tag{16}$

Nusselt number and Skin friction are given by [19]

$$Nu_1 = \frac{k_{hnl}}{k_l}\left(\frac{d\theta}{dR)}\right)_{R=1}, \tau_1 = \frac{\mu_{hnl}}{\mu_1}\left(\frac{dU}{dR}\right)_{R=1}, \; at\, R = 1$$

$$Nu_\lambda = \frac{k_{hnl}}{k_l}\left(\frac{d\theta}{dR)}\right)_{R=\lambda}, \tau_l = \frac{\mu_{hnl}}{\mu_l}\left(\frac{dU}{dR}\right)_{R=\lambda}, \; at\, R = \lambda \tag{17}$$

The dimensionless quantities obtained from Eqs. (13)-(16) are given below:

$Mc = \frac{g(\rho\beta_0)_l(T_w-T_0)a^2}{u_0\mu_l}$ (mixed convection parameter), $Qc = \frac{(\rho\beta_1)_l}{(\rho\beta_0)_l}(T_w - T_0)$ (quadratic convection parameter), α is the angle of inclination, $Da = \frac{K}{a^2}$ (Darcy number), $Q_T = \frac{Q_0 a^2}{v_l(\rho C_p)_l}$ (temperature-related heat source parameter), $Bi_1 = \frac{h_1 a}{k_l}$ and $Bi_2 = \frac{h_2 a}{k_l}$ (Boit number for each cylinder), $Re = \frac{u_0 a}{v_l}$ (Reynolds number), $Pr = \frac{(\mu C_p)_l}{k_l}$ is the Prandtl number, $\lambda = \frac{b}{a}$ (aspect ratio).

$A_1 = \frac{1}{(1-\emptyset)^{2.5}}$, $A_2 = (1-\emptyset) + \emptyset_{Cu}\frac{(\rho\beta_0)_{Cu}}{(\rho\beta_0)_l} + \emptyset_{Au}\frac{(\rho\beta_0)_{Au}}{(\rho\beta_0)_l}$

$$A_3 = (1 - \emptyset) + \emptyset_{Cu}\frac{(\rho)_{Cu}}{(\rho)_l} + \emptyset_{A_u}\frac{(\rho)_{Au}}{(\rho)_l}$$

$$A_4 = \frac{\left(\frac{(\emptyset k)_{Cu} + (\emptyset k)_{Au}}{\emptyset}\right) + (m-1)k_l + (m-1)((\emptyset k)_{Cu} + (\emptyset k)_{Au}) - (m-1)k_l\emptyset}{\left(\frac{(\emptyset k)_{Cu} + (\emptyset k)_{Au}}{\emptyset}\right) + (m-1)k_l - ((\emptyset k)_{Cu} + (\emptyset k)_{Au}) + k_l\emptyset} \; and \; \frac{dP}{dZ} = M$$

Table 1: EO, Cu and Au nanoparticles thermos-physical properties at 300K

Properties	Cu	Au	EO	Shape of Nanoparticles	m
Density $(kg\,m^{-3})$	8933	19300	884	Spherical	3
Thermal conductivity $K(W\,m^{-1}k^{-1})$	401	129.1	0.144	Platelet	5.7
Thermal expansion coefficient $\beta(k^{-1})(10^{-5})$	1.67	1.80	57	Cylinder	4.8
Dynamic viscosity $\mu(kg\,m^{-1}s^{-1})$	-	-	-	Brick	3.7

Methodology:

In the view of boundary conditions (16) the governing Eqs. (13-15) are numerically solved using the finite difference method based on bvp5c algorithm. (see Shampine kierzenka [42]). By substituting $[U, \; U', \theta \;, \theta' \;, \phi \;, \phi'] = [y_1, y_2, y_3, y_4, y_5, y_6]$, the system of first order differential equations are as follows.

$$\begin{pmatrix} y_1' \\ y_2' \\ y_3' \\ y_4' \\ y_5' \\ y_6' \end{pmatrix} = \begin{pmatrix} y_2 \\ \frac{U}{D_a} + \frac{M}{A_1} - \frac{1}{R}\frac{du}{dR} - \frac{Mc}{A1}[A_2\theta + Q_c.\theta^2]cos\alpha \\ y_4 \\ \frac{-1}{R}\frac{d\theta}{dR} - Q_T\frac{\theta.Pr}{A_4} - \frac{Pr}{A_4}.Q_E.\exp(-nr) \\ y_6 \\ \frac{-1}{R}\frac{d\emptyset}{dR} + K.S_c.\phi \end{pmatrix} \quad (18)$$

and corresponding initial   conditions

$$[y_1(1), y_2(1), y_3(1), y_4(1), y_5(1), y_6(1)] = [0, t_1, t_2, \frac{Bi_1}{A_4}t_2, c_1, c_2\frac{-Di_1}{K_{nl}}c_2]$$

Where $t_1 \; and \; t_2$ are the initial guess. Here the values for the initial guess are approximated until the boundary conditions are satisfied. Besides the maximum residual 10^{-5}. Table 2 provides the documentation of the heat transfer Nu_1 values in comparison with those reported by Oni [34] for various values of $Q_T(Q_T = 0.5(0.5)3.0)$. the comparison shows an excellent collaboration.

Table 2: Numerical values of Nu_1 for change in values of Q_T when Da=0.1, Mc= 50, Pr =1, $Q_C = Q_E = \varphi = 0$ and $\alpha = 0°$.

Q_r	Oni [8]	Present work
0.5	1.571404	1.571404
1.0	1.716981	1.716981
1.5	1.882604	1.882604
2.0	2.072277	2.072277
2.5	2.291116	2.291116
3.0	2.545765	2.545765

Results and Discussions:
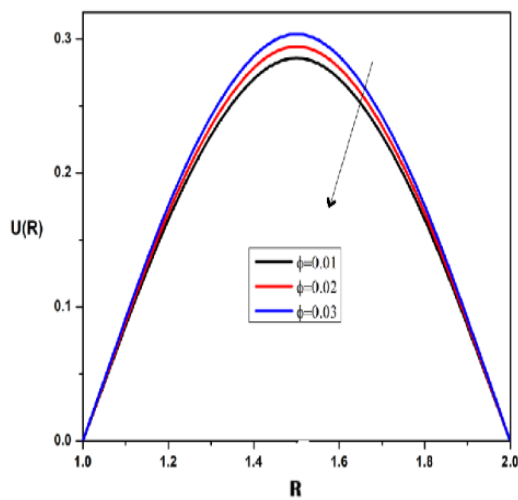
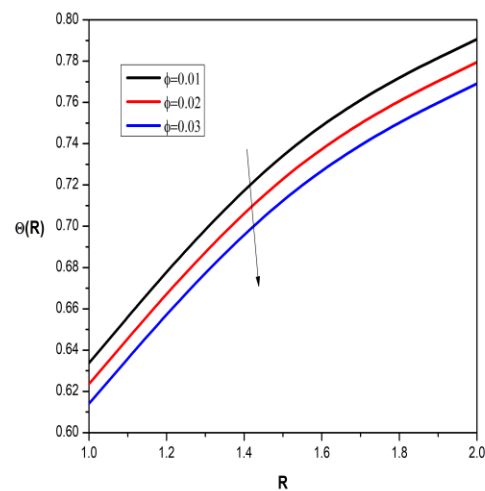
Fig 2: $\emptyset$ influence on U(R)
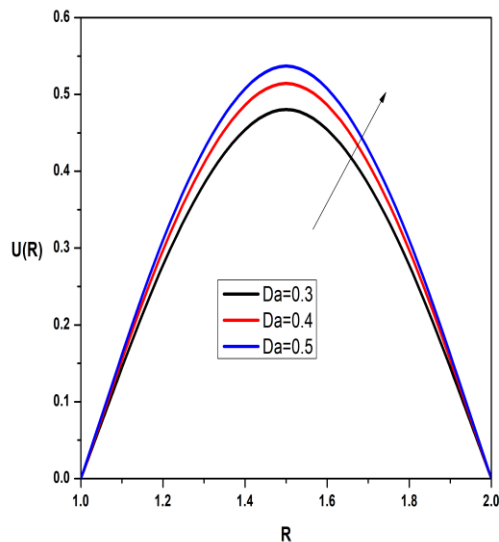

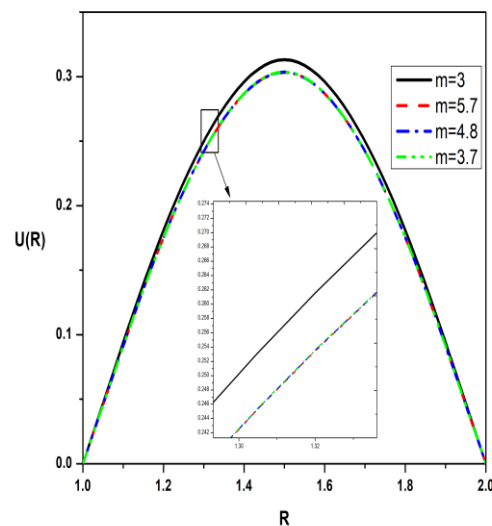Fig 3: $\emptyset$ influence on $\theta(R)$

Fig 4: D_a influence on U(R)

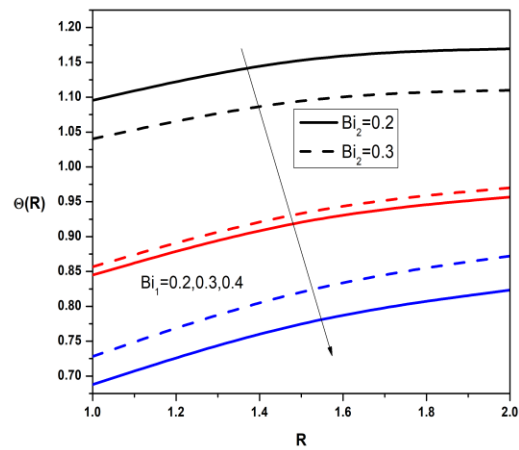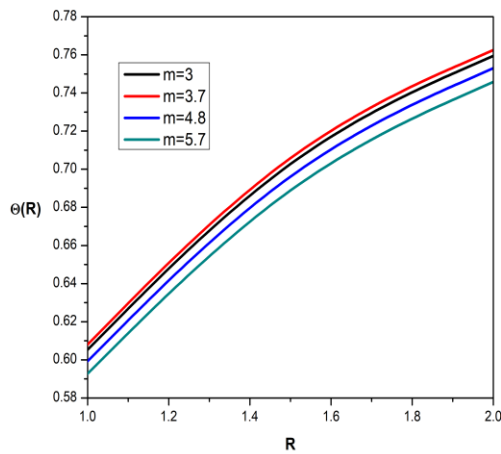Fig 5: the shape of the nanoparticle influence on U (R)

Fig 6: the shape of the nanoparticle influence   Fig 7: Bi_1 and Bi_2 influence on θ (R)
on θ (R)

Graphs and tables are used to analyze the nature of velocity U(R), temperature θ(R), skin friction coefficients (τ₁ & τλ), and heat transfer rate (Nu_1 & Nu_λ) for changes in the values of mixed convection parameter (Mc), angle of inclination (α), quadratic convection parameter (Qc), THS parameter (Q_T), ESHS parameter (Q_E), Darcy number (Da), Biot number for each cylinder (Bi_1 & Bi_2), and total nanoparticle volume fraction ($\emptyset$).The effective parameters values for these graphs and tables are fixed as follows: Mc = 2, Qc = 0.5, a = π/4, Da = 0.1, Q_T =0.01, Q_E = 0.1, $Bi_1 = Bi_2$ = 0.3, Pr = 6.0674, and $\emptyset$= 4%.

Parametric analysis

The response of total nanoparticles volume fraction $\emptyset$ on the U(R) is displayed in Fig. 2. As $\emptyset$ increases, the magnitude of U(R) decreases. In a physical sense, the suspension of nanoparticles in a transparent liquid increases the base liquid's density and makes it denser, which lowers the liquid's velocity in an inclined porous annulus.Near the inner and outer cylinders, an increase in $\emptyset$ results in an improvement and a decrease in θ(R). as shown in Fig 3. The behavior of the velocity field for the various value of Da is illustrated in Fig. 4. For the lower value of Da, the permeability is tiny or the porous matrix is densely packed. Here, a greater value of Da causes the frictional drag to decrease, improving the velocity in the porous region (Da ≠ 0) as opposed to the clear hybrid nanoliquid region (Da = 0). Our findings for Da are comparable to Oni's [34].

The relevance of nanoparticle shape aspect on U(R) is sketched in Fig. 5. Platelet-shaped nanoparticles had the highest U(R), followed by cylinder, brick, and spherical-shaped nanoparticles. Fig 6. shows the variation in θ(R) for the different shapes of nanoparticles. Near the inner cylinder, platelet-shaped nanoparticles have a higher temperature profile than cylinder, brick, and spherical-shaped nanoparticles; however, the opposite is true near the outer cylinder, and increase in $\emptyset$ results in an improvement in θ(R) near the inner cylinder and a decrease in θ(R) toward the outside cylinder. The fact that the point of junction took place inside the annulus suggests that $\emptyset$ has no discernible effect on θ(R).

The consequence of Bi, and Bi_2 on U(R) is displayed in Fig. 7. At the two cylinders, $Bi_1 \neq Bi_2$, separate heat transfer coefficients $h_1 and, h_2$ are measured. The 2D graph shows that for an increasing value of Bi_1 and Bi_2, the U(R) decreases and improves proportionally.

This is due to the fact that a higher Biot number increases the rate of heat transfer at the cylinder walls. The influence of Bi_1 and Bi_2 on $\theta(R)$ is diagrammed in Fig. 7. When the value of Bin increases, the temperature distribution improves, but when Bi_1 increases, it diminishes. Convective cooling at the cylinders is the reason of this.

Conclusions

We numerically simulate the hybrid nano liquid flow with ESHS and THS in a convectively heated inclined annulus. The following are the primary results of this work:
• The mixed and quadratic convection mechanisms favour the hybrid nano liquid's momentum.
• As the angle of inclination increases, the acceleration caused by gravity has less of an impact on the flow field; the amplitude of the temperature and velocity fields increases with the heat source phenomena.
• As the Biot number increases, the outer cylinder's flow structure and thermal pattern improve.
• In contrast to the clear hybrid nano liquid area (Da = 0), the momentum structure is higher in the porous zone (Da ≠0).
• Platelet-shaped nanoparticles have the highest velocity and temperature fields, followed by cylinder, brick, and spherical-shaped nanoparticles.
• THS and ESHS have positive effects on heat transmission and the friction factor.
• The rise in friction at the cylinder walls is responsible for the quadratic convection, mixed convection, and Darcy number.
• THS has a greater influence on the local Nusselt number than the total nanoparticle volume percentage.
• The sensitivity of the Nusselt number Nu_1 to the concentration of nanoparticles, ESHS, and THS is positive.

References:
[1] S.U.S. Choi, J.A. Eastman, Enhancing thermal conductivity of fluids with nanoparticles, ASME Int. Mech. Eng. Cong. Expos. 66 (1995) 99-105.
[2] R.X. Yin, DZ. Yang, JZ Wu, Nanoparticle drug and gene-eluting stents for the prevention and treatment of coronary restenosis, Theranostics 4 (2014) 175-200.
[3] R.K. Tiwari, M.K. Das, Heat transfer augmentation in a two-sided lid-driven differentially heated square cavity utilizing nanofluids, Int. J. Heat Mass Transf. 50 (2007) 2002-2018.
[4] N.S. Akbar, Metallic nanoparticles analysis for the peristaltic flow in an asymmetric channel with MHD, IEEE Trans. Nanotechnol. 13 (2014) 357-361.
[5] S. Nadeem, 1. Shahzadi, Mathematical analysis for peristaltic flow of two phase • nanofluid in a curved channel, Commun. Theor. Phys. 64 (2015) 547-554.
[6] S. Nadeem, S. Ijaz, Impulsion of nanoparticles as a drug carrier for the theoretical investigation of stenosed arteries with induced magnetic effects, J. Magn. Magn. Mater. 410 (2016) 230-241.
[7] T. Hayat, T. Muhammad, S.A. Shehzad, A. Alsaedi, On three-dimensional boundary layer flow of Sisko nanofluid with magnetic field effects, Adv. Powder Technol. 27 (2016) 504-512.
[8] D.S. Sankar, K. Hemalatha, A non-Newtonian fluid flow model for blood flow through a catheterized artery-steady flow, Appl. Math. Model. 31 (2007) 1847.

[9] K.S. Mekheimer, Y.A. Elmaboud, The influence of heat transfer and magnetic field on peristaltic transport of a Newtonian fluid in a vertical annulus: application of an en-doscope, Phys. Lett. A 372 (2008) 1657.

[10] S. Suresh K.P. Venkitaraj. P. Selvakumar, M. Chandrashekar, Effect of Al2O3-Cu/water hybrid nanofluid in heat transfer, Exp. Thermal Fluid Sci. 38(2012) 54-60.

[11] S.S.U. Devi, Numerical investigation of three-dimensional hybrid Cu-Al2O3/water nanofluid flow over a stretching sheet with effecting Lorentz Force subject to Newtonian heating, Can. J. Phys. 94(5) (2016) 490-496.

[12] C. Kanchana, P. G. Siddheshwar, Y. Zhao, A study of Rayleigh-Benard convection in hybrid nanoliquids with physically realistic boundaries, Europ. Physical J. Special Topics 228(12) (2019) 2511-2530.

[13] B. Venkateswarlu, Satya Narayana, P. V., Cu-Al2O3/H2O hybrid nanofluid flow past a porous stretching sheet due to temperature dependent viscosity ans viscous dissipation, Heat Trans. (2020), https://doi.org/10.1002/htj.21884.

[14] I. Waini, A. Ishak, T. Grosan, I. Pop, Mixed convection of a hybrid nanofluid flow along a vertical surface embedded in a porous medium, Int. Commun. Heat Mass Trans. 144(2020) 104565.

[15] A.J. Chamkha, Heat and mass transfer from MHD flow over a moving permeable cylinder with heat generation or absorption and chemical reaction, Commun. Numer. Anal. 2011 (2011) 20, http://dx.doi.org/10.5899/ cna-00109. Article ID cna-00109.

[16] M.A. Hossain, M. Kuttubuddin, I. Pop. Radiation-conduction interaction on mixed convection from a horizontal circular cylinder, Int. J Heat Mass Transfer 35 (1999) 307-314.

[17] M. O. Oni, Combined effect on heat source, porosity and thermal radiation on mixed convection flow in vertical annulus an exact solution, Eng. Sci. Technol. Int. J. 20(2) (2017)518-527.

[18] P.K. Kameswaran, B. Vasu, P.V.S.N Murthy, R.S.R. Gorla, Mixed convection from a wavy surface embedded in a thermally stratified nanofluid saturated porous medium with non-linear Boussinesq approximation, Int. Commun. Heat Mass Trans. 77(2016) 78-86.

[19] K. Thriveni, B. Mahanthesh, Nonlinear Boussinesq buoyancy driven flow and radiative heat transport of magneto hybrid nanoliquid in an annulus: a statistical framework, Heat Trans. 49(8) (2020) 4759-4782.

[20] N. Nalinakshi, P. A. Dinesh, and D. V. Chandrashekar, "Numerical Study of Double Diffusive Mixed Convection with Variable Fluid Properties", International Journal of Engineering Research & Technology (IJERT), Vol. 2 Issue 9, September - 2013. ISSN: 2278-018.

[21] Mahesha R, Nalinakshi N, Sravan kumar T and Sreenivasa T N, "Thermal Radiation-Driven MHD Nanofluid Flow in a Concentric Cylinder concerning cancer therapy", Periodico di Mineralogia, Vol. 93(6), 148-161, 2024 **DOI: https://doi.org/10.5281/zenodo.14172363**

[22] Sowmya S B, Nalinakshi N and Sreenivasa T N, "Effects of Magnetic Field and Ohmic Heating on Mixed Convection over a Vertical Heated Plate" Periodico di Mineralogia, Vol. 93(6), 303-319, 2024 DOI: https://doi.org/10.5281/zenodo.14227176